Liquid Crystals
Publication details, including instructions for authors and subscription information:
http://www.informaworld.com/smpp/title~content=t713926090

Synthesis and thermal properties of dimeric alkoxy-substituted tolans

Igor L. Rozhanskii[a,b]; Ikuyoshi Tomita[a]; Takeshi Endo[a]
[a] Research Laboratory of Resources Utilization, Tokyo Institute of Technology, Yokohama, Japan [b] Tsukuba Research Laboratory, Japan Synthetic Rubber Ltd., Tsukuba, Ibaraki, Japan.

To cite this Article Rozhanskii, Igor L. , Tomita, Ikuyoshi and Endo, Takeshi(1996) 'Synthesis and thermal properties of dimeric alkoxy-substituted tolans', Liquid Crystals, 21: 5, 631 — 643

To link to this Article: DOI: 10.1080/02678299608032875

URL: http://dx.doi.org/10.1080/02678299608032875

LIQUID CRYSTALS, 1996, VOL. 21, NO. 5, 631–643

Synthesis and thermal properties of dimeric alkoxy-substituted tolans

by IGOR L. ROZHANSKII†, IKUYOSHI TOMITA and TAKESHI ENDO*
Research Laboratory of Resources Utilization, Tokyo Institute of Technology,
4259 Nagatsuta, Midori-ku, Yokohama 226, Japan

(Received 18 April 1996; accepted 25 May 1996)

Four homologous series of dimeric tolans of the general formula $RC_6H_4C{\equiv}CC_6H_4O(CH_2)_mOC_6H_4C{\equiv}CC_6H_4R$ ($m=6$–10; $R=H$, OC_6H_{13}, $OC_{10}H_{21}$ and $OC_{14}H_{29}$), denoted further as TO*m*OT or *n*OTO*m*OTO*n*, according to the number of aliphatic carbon atoms, have been synthesized. Dimers with terminal chains exhibited liquid crystalline behaviour. Crystal–crystal transitions were also observed. Resulting from the optical, thermal and miscibility studies, the following mesophases have been identified: nematic, smectics A and B, and the tilted smectics C and (probably) F or I. In the 6OTO*m*OTO6 series, a phase with a strong tendency to self-alignment occurred between the nematic and smectic A phases. This phase resembled the nematic in its viscoelastic properties, but also showed focal-conic textures. A transition between this 'intermediate phase' and the nematic was detected only from microscopic observations. On the contrary, the 'intermediate phase'–smectic A transition was also detected by DSC ($\Delta H \sim 1\,\mathrm{kJ\,mol^{-1}}$). Both tilted ($S_C$ and $S_{F/I}$) and non-tilted (S_A and S_B) smectics were observed in the 10OTO*m*OTO10 series, while only tilted smectic phases were identified in the dimers with longer terminal substituents (14OTO*m*OTO14). Double melting behaviour was found in 14OTO8OTO14 and 14OTO10OTO14. An alternation of the transition temperatures and enthalpies with the odd–even alternation of the lengths of bridging groups was clearly observed. A correlation between total enthalpies of transition and solubilities of the dimeric tolans is stated.

1. Introduction

In recent years, many compounds consisting of two mesogenic units connected by a flexible spacer have been studied. Such an interest in them appeared firstly due to their structural similarity to semi-rigid main-chain polymeric liquid crystals [1, 2]. They were also regarded as convenient model compounds for the conformational study of methylene chains [3, 4]. Furthermore, many liquid crystalline dimers exhibited quite different properties to conventional low molar mass liquid crystals. Some dimesogens exhibited some rare mesophases, such as biaxial nematics in discotic–discotic twins [5] or incommensurate smectics in unsymmetric calamitic–cholesteric dimers [6, 7]. A rich smectic polymorphism was found in dimeric liquid crystals with alkoxybenzylidene mesogenic units [8].

In this work, four homologous series of symmetric dimers bearing tolan (diphenylacetylene) units connected via linear aliphatic alkoxy groups were synthesized and studied by thermal and optical methods. These dimeric tolans were obtained as intermediate compounds for the synthesis of (η^5-cyclopentadienyl)(η^4-cyclobutadiene)-cobalt-containing polymers having discotic organometallic cores and flexible bridging groups [9]. During the synthesis and characterization of the required tolans, their complicated thermal behaviour was found. To the best of our knowledge, dimeric liquid crystals with tolan units have not been previously reported.

The analogous monomeric tolans with linear alkyl, alkoxy or alkanoate substituents were first prepared in the early 1970s [10, 11]. Most of the monomeric species exhibited nematic phases, starting from tolans with pentyl (or pentyloxy) substituents. Smectic phases (S_A and S_C) were found in 4,4′-bis(*n*-decyloxy)tolan [10]. Similarly, main-chain tolan-containing polymers with linear alkyl [12] or alkanoyl [13, 14] spacers exhibited nematic phases. Tolan-containing polyesters [14] formed smectic phases when the spacer contained 8 or 10 methylene groups. An odd–even alternation of both the crystal–mesophase and mesophase–isotropic transition temperatures was also observed, the values for the homologues with their lowering with an odd number of methylene groups in the spacer falling on a lower curve. The mesophase temperature range lessened as the length of the spacer increased.

---

*Author for correspondence.

†Present address: Tsukuba Research Laboratory, Japan Synthetic Rubber Ltd., 25 Miyukigaoka, Tsukuba, Ibaraki 305 Japan.

0267–8292/96 $12·00 © 1996 Taylor & Francis Ltd.

2. Experimental

2.1. *Materials and instruments*

Trimethylsilylacetylene was synthesized following the literature procedure [15]. Tetrahydrofuran (THF) was dried over sodium and distilled under nitrogen before use. All other materials were obtained from Tokyo Kasei Co. and used as received. ^{1}H NMR spectra were recorded on a JEOL JNM-PMX60si NMR spectrometer, using $CDCl_3$ as a solvent (tetramethylsilane as an internal standard). Infrared spectra were obtained on a Jasco FT/IR-5300 spectrophotometer, both in neat samples and KBr disks. Differential scanning calorimetry (DSC) measurements were carried out on a Seiko Instruments SSC/5200 calorimeter, calibrated with an indium (99·999 per cent) standard. Samples of between 5–7 mg and scanning rates of 5°C min^{-1} were used. In a number of analyses, heating–cooling rates varied from 20 to 1°C min^{-1} in order to study the effect on the transitional properties. Slow scanning rates (0·5–1°C min^{-1}) and bigger samples (10–20 mg) were used when weak transitions were observed or expected. The detection limit was *c.* 0·1 J g^{-1}, corresponding to $\Delta H_{trans} \approx 75$–120 J mol^{-1}. Transition temperatures were rounded to the nearest 0·5°C, averaged from several independent measurements. Transition enthalpies and entropies were determined with a precision of between 5–7 per cent, and were correspondingly rounded. Polarizing microscopic observations were performed on a Olympus BH-2 microscope equipped with a Mettler FP90 hot stage. Isotropic melts of samples were placed between clean glass slides and then were cooled down to the desired temperatures. The thickness of the films varied from *c.* 2 to 50 µm. Uncovered free droplets were also studied. The solubility of the tolans in chloroform was measured at 20°C according to the following technique: a weighed sample was placed into a tightly sealed flask equipped with a magnetic stirrer bar. Portions of chloroform were gradually added with a pipette to the stirred solution until most of the sample was dissolved. The mixture was then stirred for an additional 3–4 h. The stirring was stopped, the insoluble part allowed to precipitate and the clear solution decanted into a weighed one-necked flask. The solvent was removed under reduced pressure and the solubility was calculated according to the weight of the soluble part and a volume of added chloroform.

2.2. *Synthesis*

The general procedure is given in scheme 1. As an example, the synthesis of 1,6-bis(4-(phenylethynyl)phenoxy)hexane (TO6OT) and 1,6-bis(4-(4′-*n*-decyloxy-

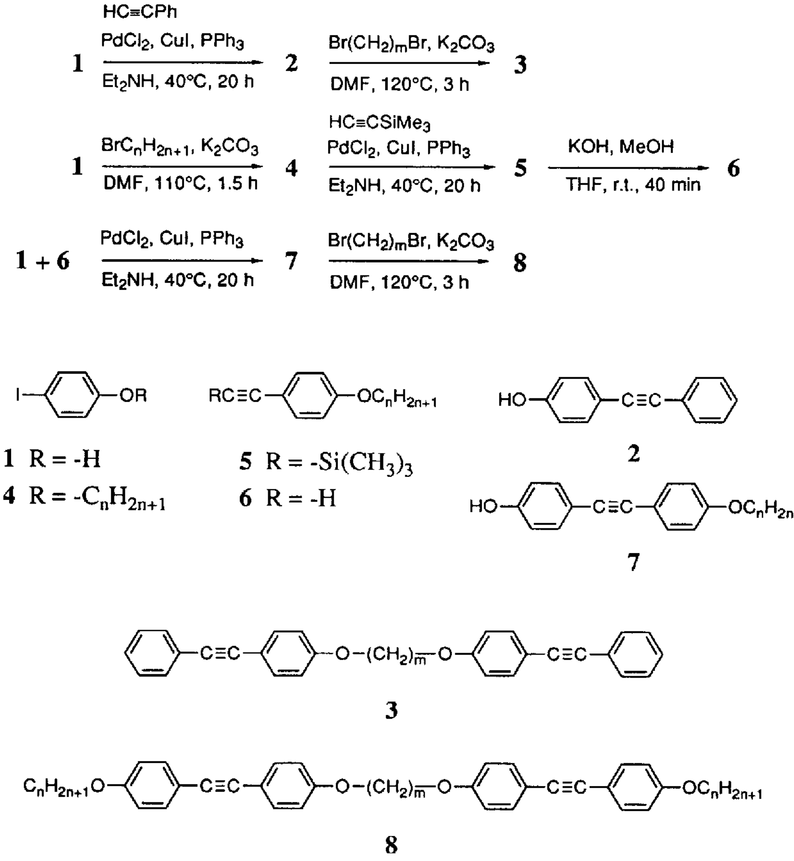

Scheme 1.

phenylethynyl)phenoxy)hexane (10OTO6OTO10) are described. Compounds of the corresponding series were obtained similarly.

2.2.1. *(4-Phenylethynyl)phenol (2)*

p-Iodophenol (**1**) (4·40 g, 20 mmol), phenylacetylene (2·55 g, 25 mmol), $PdCl_2$ (36 mg, 0·8 mol %), CuI (18 mg, 0·4 mol %), triphenyphosphine (215 mg, 4·0 mol %) and diethylamine (65 ml) were placed into a two-necked 200 ml flask equipped with a reflux condenser and magnetic stirrer bar under nitrogen. The reaction mixture was stirred overnight at 40–45°C. After the removal of the solvent under reduced pressure, the residue was treated with 200 ml of 1 M HCL and extracted four times with diethyl ether (100 ml). After drying over Na_2SO_4 and reducing the volume of the organic phase, the final product (**2**) was isolated by column chromatography (SiO_2, benzene). The resulting pale-yellow powder was recrystallized from benzene as colourless crystals (m.p. 122–123°C, literature 123–125°C [16]). Yield: 3·25 g (84 per cent). ^{1}H NMR (δ/ppm): 6·72–7·30 (C_6H_4, C_6H_5). IR (KBr, cm^{-1}): 3422 (–OH), 3054 (C–H aromatic), 1609, 1591, 1510 (C=C), 1252 (C–O), 833, 799, 750, 689 (=C–H out-of-plane).

2.2.2. *α,ω-Bis(4-(phenylethynyl)phenoxy)alkanes (3)*

1,6-Bis(4-(phenylethynyl)phenoxy)hexane (TO6OT). **2** (860 mg, 4·4 mmol), 1,6-dibromohexane (488 mg, 2·0 mmol), K_2CO_3 (1·5 g) and DMF (10 ml) were placed into a one-necked 50 ml flask equipped with a reflux condenser and a magnetic stirrer bar. The mixture was stirred at 120–125°C for 3 h, poured into 200 ml of 1 M aqueous NaOH and the resulting suspension stirred for 30 min. The precipitate was filtered, washed repeatedly with water and then methanol. The final product was recrystallized from dichloromethane–methanol as greenish mica-like crystals. Yield: 800 mg (85 per cent). ^{1}H NMR (δ/ppm): 1·55 (–CH_2–, 8 H), 4·00 (t, –O–CH_2–, 4 H), 6·82–7·50 (C_6H_4, C_6H_5, 18 H). IR (KBr, cm^{-1}): 3048 (C–H aromatic), 2942, 2866 (C–H aliphatic), 1607, 1590, 1519 (C=C), 1246 (C–O), 839, 806, 750, 691 (=C–H out-of-plane).

1,7-Bis(4-(phenylethynyl)phenoxy)heptane (TO7OT). Colourless mica-like crystals from chloroform–methanol. Yield: 41 per cent. ^{1}H NMR (δ/ppm): 1·30 (–CH_2–, 10 H), 4·00 (t, –O–CH_2–, 4 H), 6·82–7·50 (C_6H_4, C_6H_5, 18 H). IR (KBr, cm^{-1}): 3050, 2934, 2849, 1607, 1595, 1512, 1244, 837, 812, 756, 689.

1,8-Bis(40(phenylethynyl)phenoxy)octane (TO8OT). Colourless mica-like crystals from chloroform–methanol. Yield: 53 per cent. ^{1}H NMR (δ/ppm): 1·30 (–CH_2–, 12 H), 4·00 (t, –O–CH_2–, 4 H), 6·82–7·50 (C_6H_4, C_6H_5, 18 H). IR (KBr, cm^{-1}): 3050, 2938, 2861, 1607, 1595, 1512, 1248, 839, 826, 801, 750, 691.

1,9-Bis(4-(phenylethynyl)phenoxy)nonane (TO9OT). Greenish mica-like crystals from chloroform–methanol. Yield: 50 per cent. ^{1}H NMR (δ/ppm): 1·30 (–CH_2–, 14 H), 4·00 (t, –O–CH_2–, 4 H), 6·82–7·50 (C_6H_4, C_6H_5, 18 H). IR (KBr, cm^{-1}): 3052, 2932, 2851, 1605, 1595, 1512, 1244, 837, 810, 756, 689.

1,10-Bis(4-(phenylethynyl)phenoxy)decane (TO10OT). Greenish mica-like crystals from chloroform. Yield: 65 per cent. ^{1}H NMR (δ/ppm): 1·30 (–CH_2–, 16 H), 4·00 (t, –O–CH_2–, 4 H), 6·82–7·50 (C_6H_4, C_6H_5, 18 H). IR (KBr, cm^{-1}): 3050, 2936, 2922, 2853, 1607, 1595, 1510, 1250, 839, 829, 802, 752, 691.

2.2.3. *1-n-Decyloxy-4-iodobenzene (4, n = 10)*

p-Iodophenol (**1**) (6·16 g, 28 mmol), 1-bromodecane (6·00 g, 27 mmol), K_2CO_3 (12 g) and DMF (70 ml) were placed in a one-necked 200 ml flask equipped with a reflux condenser and a magnetic stirrer bar. The mixture was kept stirring at 110–120°C for 1·5 h, then was poured into 1200 ml of 1 M NaOH. The resulting suspension was stirred for 30 min and was then extracted four times with *n*-hexane (100 ml). After drying over Na_2SO_4 and reducing the volume, the organic phase was purified by column chromatography (SiO_2, hexane : diethyl ether = 5 : 1). The final product was isolated as a pale-yellow viscous liquid. Yield: 8·64 g (89 per cent). ^{1}H NMR (δ/ppm): 0·88 (t, –CH_3, 3 H), 1·30 (–CH_2–, 16 H), 3·82 (t, –O–CH_2–, 2 H), 6·50–7·50 (C_6H_4, 4 H). IR (neat, cm^{-1}): 2924, 2855 (C–H aliphatic), 1588, 1487 (C=C), 1244 (C–O), 820 (=C–H out-of-plane).

1-n-Hexyloxy-4-iodobenzene (**4**, *n* = 6). Pale-yellow viscous liquid. Yield: 84 per cent. ^{1}H NMR (δ/ppm): 0·88 (t, –CH_3, 3 H), 1·30 (–CH_2–, 8 H), 3·82 (t, –O–CH_2–, 2 H), 6·50–7·50 (C_6H_4, 4 H). IR (neat, cm^{-1}): 2932, 2860, 1588, 1487, 1244, 820.

1-n-Tetradecyloxy-4-iodobenzene (**4**, *n* = 14). Colourless crystals (m.p. 44·5–45·5°C). Yield: 88 per cent. ^{1}H NMR (δ/ppm): 0·88 (t, –CH_3, 3 H), 1·30 (–CH_2–, 24 H), 3·82 (t, –O–CH_2–, 2 H), 6·50–7·50 (C_6H_4, 4 H). IR (KBr, cm^{-1}): 2924, 2855, 1588, 1487, 1244, 820.

2.2.4. *1-(4-n-Decyloxyphenyl)-2-(trimethylsilyl) acetylene (5, n = 10)*

Compounds **5** were prepared by the modification of the Sonogashira method [17]. **4** (*n* = 10, 8·64 g, 24 mmol), $PdCl_2$ (48 mg, 1·0 mol %), CuI (24 mg, 0·5 mol %), triphenylphosphine (290 mg, 4·5 mol %) and diethylamine (85 ml) were placed into a two-necked 200 ml flask equipped with a reflux condenser and a magnetic stirrer bar under nitrogen. The mixture was stirred at reflux for 40 min, then cooled to 45°C. Trimethylsilyacetylene (2·94 g, 30 mmol) was added dropwise via a syringe and the reaction mixture was stirred overnight at 40–45°C. After the removal of the solvent under reduced pressure the residue was treated with 200 ml diethyl ether, and the insoluble diethylammonium iodide removed by filtration. After reducing the volume of the filtrate, the final product was isolated by the column chromatography (SiO_2, hexane : diethyl ether = 5 : 1) as a pale-yellow wax-like solid. Yield: 6·73 g (91 per cent). ^1H NMR (δ/ppm): 0·20 (s, Si–CH_3, 9 H), 0·88 (t, –CH_3, 3 H), 1·30 (–CH_2–, 16 H), 3·85 (t, –O–CH_2–, 2 H), 6·60–7·35 (C_6H_4, 4 H). IR (neat, cm^{-1}): 2927, 2855 (C–H aliphatic), 2157 (C≡C), 1605, 1507 (C=C), 1248 (C–O), 866, 841, 760 (–Si(CH_3)$_3$ and =C–H out-of-plane).

1-(4-n-Hexyloxyphenyl)-2-(trimethylsilyl)acetylene (**5**, $n = 6$). Yellow oily liquid. Yield: 93 per cent. ^1H NMR (δ/ppm): 0·20 (s, Si–CH_3, 9 H), 0·88 (t, –CH_3, 3 H), 1·30 (–CH_2–, 8 H), 3·85 (t, –O–CH_2–, 2 H), 6·60–7·35 (C_6H_4, 4 H). IR (neat, cm^{-1}): 2957, 2934, 2861, 2157, 1605, 1507, 1248, 866, 841, 760.

1-(4-n-Tetradecyloxyphenyl)-2-(trimethylsilyl)acetylene (**5**, $n = 14$). Pale-yellow wax-like solid. Yield: 92 per cent. ^1H NMR (δ/ppm): 0·20 (s, Si–CH_3, 9 H), 0·88 (t, –CH_3, 3 H), 1·30 (–CH_2–, 24 H), 3·85 (t, –O–CH_2–, 2 H), 6·60–7·35 (C_6H_4, 4 H). IR (KBr, cm^{-1}): 2927, 2855, 2157, 1605, 1507, 1248, 866, 841, 760.

2.2.5. *(4-n-Decyloxyphenyl)acetylene (6, n = 10)*

5 ($n = 10$, 6·73 g, 22 mmol) was placed into a one-necked 200 ml flask equipped with a magnetic stirrer bar and was dissolved in 50 ml of THF under nitrogen. 25 ml of 1·5 M KOH solution in methanol were added, and the reaction mixture stirred at room temperature for 40 min. The solvent was removed by rotary evaporation and the residue treated with 300 ml of 10 per cent aqueous $NaHCO_3$. The resulting suspension was extracted four times with diethyl ether (100 ml). After drying over Na_2SO_4, the collected organic phase was concentrated under reduced pressure and the final product isolated by column chromatography (SiO_2, hexane : benzene = 4 : 1) as a pale-yellow viscous liquid. Yield: 5·56 g (98 per cent). ^1H NMR (δ/ppm): 0·88 (t, –CH_3, 3 H), 1·30 (–CH_2–, 16 H), 2·93 (s, ≡CH, 1 H), 3·90 (t, –O–CH_2–, 2 H), 6·68–7·40 (C_6H_4, 4 H). IR (neat, cm^{-1}): 3318, 3293 (≡C–H), 2927, 2855 (C–H aliphatic), 2108 (C≡C), 1607, 1507 (C=C), 1248 (C–O), 831 (=C–H out-of-plane).

(4-n-Hexyloxyphenyl)acetylene (**6**, $n = 6$). Yellow oily liquid. Yield: 98 per cent. ^1H NMR (δ/ppm): 0·88 (t, –CH_3, 3 H), 1·30 (–CH_2–, 8 H), 2·93 (s, ≡CH, 1 H), 3·90 (t, –O–CH_2–, 2 H), 6·68–7·40 (C_6H_4, 4 H). IR (neat, cm^{-1}): 3316, 3293, 2934, 2870, 2108, 1607, 1507, 1250, 833.

(4-n-Tetradecyloxyphenyl)acetylene (**6**, $n = 14$). Colourless crystals (m.p. 34–35°C). Yield: 98 per cent. ^1H NMR (δ/ppm): 0·88 (t, –CH_3, 3 H), 1·30 (–CH_2–, 24 H), 2·93 (s, ≡CH, 1 H), 3·90 (t, –O–CH_2–, 2 H), 6·68–7·40 (C_6H_4, 4 H). IR (KBr, cm^{-1}): 3316, 3289, 2919, 2849, 2108, 1607, 1509, 1252, 839.

2.2.6. *4-(4′-n-Decyloxyphenylethynyl)phenol (7, n = 10).*

p-Iodophenol (**1**) (3·75 g, 17 mmol), $PdCl_2$ (30 mg, 1·0 mol %), CuI (15 mg, 0·5 mol %), triphenyphosphine (180 mg, 4·5 mol %) and diethylamine (35 ml) were placed into a two-necked 200 ml flask equipped with a reflux condenser and magnetic stirrer bar under nitrogen. The reaction mixture was stirred at reflux for 40 min and then was cooled. A solution of **6** ($n = 10$, 5·28 g, 20·5 mmol) in 30 ml of diethylamine was added via a syringe, and the reaction mixture stirred overnight at 40–45°C. After the removal of the solvent by rotary evaporation the residue was treated with 200 ml of diethyl ether, and the insoluble diethylammonium iodide removed by filtration. After reducing the volume of the filtrate, the final product was isolated by column chromatography (SiO_2, diethyl ether:benzene = 1 : 4). The resulting yellow powder was recrystallized from benzene as colourless crystals (m.p. 111·5–112°C). Yield: 2·39 g (40 per cent). ^1H NMR (δ/ppm): 0·88 (t, –CH_3, 3 H), 1·30 (–CH_2–, 16 H), 3·93 (t, –O–CH_2–, 2 H), 4·90 (s, –OH, 1 H), 6·65–7·43 (C_6H_4, 8 H). IR (KBr, cm^{-1}): 3430 (O–H), 2921, 2853 (C–H aliphatic), 1611, 1520 (C=C), 1252 (C–O), 833 (=C–H out-of-plane).

4-(4′-n-Hexyloxyphenylethynyl)phenol (**7**, $n = 6$). Brownish-white crystals from *n*-hexane–chloroform (m.p. 113–113·5°C). Yield: 53 per cent. ^1H NMR (δ/ppm): 0·88 (t, –CH_3, 3 H), 1·30 (–CH_2–, 8 H), 3·93 (t, –O–CH_2–, 2 H), 4·90 (s, –OH, 1 H), 6·65–7·43 (C_6H_4, 8 H). IR (KBr, cm^{-1}): 3430, 2934, 2870, 1611, 1520, 1252, 833.

4-(4′-n-Tetradecyloxyphenylethynyl)phenol (**7**, $n = 14$). Colourless crystals from benzene (m.p. 117–117·5°C). Yield: 51 per cent. ^1H NMR (δ/ppm): 0·88 (t, –CH_3, 3 H), 1·30 (–CH_2–, 16 H), 3·93 (t, –O–CH_2–, 2 H), 4·85 (s, –OH, 1 H), 6·65–7·43 (C_6H_4, 8 H). IR (KBr, cm^{-1}): 3400, 2917, 2851, 1611, 1522, 1252, 833.

2.2.7. α, ω-*Bis(4-(4′-n-alkoxyphenylethynyl)phenoxy) alkanes (8)*

1,6-Bis(4-(4′-n-decyloxyphenylethynyl)phenoxy)hexane (10OTO6OTO10). **7** ($n = 10$, 385 mg, 1·1 mmol), 1,6-dibromohexane (122 mg, 0·5 mmol), K_2CO_3 (0·5 g) and DMF (4 ml) were placed into a test-tube equipped with a reflux condenser and a magnetic stirrer bar. The mixture was kept stirring at 120–125°C for 3 h, was then poured into 100 ml of 1 M NaOH and resulting suspension stirred vigorously for 30 min. The precipitate was filtered, washed repeatedly with water, then methanol and diethyl ether. The final product was recrystallized from chloroform as fine colourless crystals. Yield: 268 mg (69 per cent). ^1H NMR (δ/ppm): 0·88 (t, –CH_3, 6 H), 1·30 (–CH_2–, 40 H), 3·95 (t, –O–CH_2–, 8 H), 6·75–7·50

(C_6H_4, 16 H). IR (KBr, cm^{-1}): 2938, 2922, 2853 (C–H aliphatic), 1609, 1516 (C=C), 1250 (C–O), 839, 828, 806, 785 (=C–H out-of-plane).

1,6-Bis(4-(4′-n-hexyloxyphenylethynyl)phenoxy) hexane (6OTO6OTO6). Colourless mica-like crystals from chloroform. Yield: 59 per cent. ^1H NMR (δ/ppm): 0·88 (t, $-CH_3$, 6 H), 1·30 ($-CH_2-$, 24 H), 3·95 (t, $-O-CH_2-$, 8 H), 6·75–7·50 (C_6H_4, 16 H). IR (KBr, cm^{-1}): 2940, 2866, 1609, 1518, 1248, 839, 806, 785.

1,7-Bis(4-(4′-n-hexyloxyphenylethynyl)phenoxy) heptane (6OTO7OTO6). Colourless mica-like crystals from methanol–chloroform. Yield: 50 per cent. ^1H NMR (δ/ppm): 0·88 (t, $-CH_3$, 6 H), 1·30 ($-CH_2-$, 26 H), 3·95 (t, $-O-CH_2-$, 8 H), 6·75–7·50 (C_6H_4, 16 H). IR (KBr, cm^{-1}): 2955, 2926, 2874, 2855, 1609, 1518, 1250, 839, 824.

1,8-Bis(4-(4′-n-hexyloxyphenylethynyl)phenoxy) octane (6OTO8OTO6). Colourless fine crystals from chloroform. Yield: 40 per cent. ^1H NMR (δ/ppm): 0·88 (t, $-CH_3$, 6 H), 1·30 ($-CH_2-$, 28 H), 3·95 (t, $-O-CH_2-$, 8 H), 6·75–7·50 (C_6H_4, 16 H). IR (KBr, cm^{-1}): 2936, 2861, 1609, 1516, 1250, 839, 826.

1,9-Bis(4-(4′-n-hexyloxyphenylethynyl)phenoxy) nonane (6OTO9OTO6). Colourless mica-like crystals from methanol–chloroform. Yield: 54 per cent. ^1H NMR (δ/ppm): 0·88 (t, $-CH_3$, 6 H), 1·30 ($-CH_2-$, 30 H), 3·95 (t, $-O-CH_2-$, 8 H), 6·75–7·50 (C_6H_4, 16 H). IR (KBr, cm^{-1}): 2955, 2926, 2874, 2853, 1609, 1518, 1250, 839, 824.

1,10-Bis(4-(4′-n-hexyloxyphenylethynyl)phenoxy) decane (6OTO10OTO6). Colourless mica-like crystals from chloroform. Yield: 58 per cent. ^1H NMR (δ/ppm): 0·88 (t, $-CH_3$, 6 H), 1·30 ($-CH_2-$, 32 H), 3·95 (t, $-O-CH_2-$, 8 H), 6·75–7·50 (C_6H_4, 16 H). IR (KBr, cm^{-1}): 2955, 2925, 2859, 1609, 1518, 1248, 839, 826, 785.

1,7-Bis(4-(4′-n-decyloxyphenylethynyl)phenoxy) heptane (10OTO7OTO10). Colourless fine crystals from methanol–chloroform. Yield: 50 per cent. ^1H NMR (δ/ppm): 0·88 (t, $-CH_3$, 6 H), 1·30 ($-CH_2-$, 42 H), 3·95 (t, $-O-CH_2-$, 8 H), 6·75–7·50 (C_6H_4, 16 H). IR (KBr, cm^{-1}): 2955, 2922, 2853, 1611, 1518, 1248, 839, 826.

1,8-Bis(4-(4′-n-decyloxyphenylethynyl)phenoxy) octane (10OTO8OTO10). Colourless fine crystals from chloroform. Yield: 39 per cent. ^1H NMR (δ/ppm): 0·88 (t, $-CH_3$, 6 H), 1·30 ($-CH_2-$, 44 H), 3·95 (t, $-O-CH_2-$, 8 H), 6·75–7·50 (C_6H_4, 16 H). IR (KBr, cm^{-1}): 2936, 2920, 2853, 1609, 1516, 1248, 839, 826, 783.

1,9-Bis(4-(4′-n-decyloxyphenylethynyl)phenoxy) nonane (10OTO9OTO10). Colourless fine crystals from chloroform. Yield: 35 per cent. ^1H NMR (δ/ppm): 0·88 (t, $-CH_3$, 6 H), 1·30 ($-CH_2-$, 46 H), 3·95 (t, $-O-CH_2-$, 8 H), 6·75–7·50 (C_6H_4, 16 H). IR (KBr, cm^{-1}): 2955, 2922, 2874, 2853, 1611, 1518, 1252, 839, 826.

1,10-Bis(4-(4′-n-decyloxyphenylethynyl)phenoxy) decane (10OTO10OTO10). Colourless fine crystals from chloroform. Yield: 69 per cent. ^1H NMR (δ/ppm): 0·88 (t, $-CH_3$, 6 H), 1·30 ($-CH_2-$, 48 H), 3·95, (t, $-O-CH_2-$, 8 H), 6·75–7·50 (C_6H_4, 16 H). IR (KBr, cm^{-1}): 2955, 2922, 2853, 1609, 1518, 1250, 839, 826, 801, 785.

1,6-Bis(4-(4′-n-tetradecyloxyphenylethynyl)phenoxy) hexane (14OTO6OTO14). Colourless fine crystals from chloroform. Yield: 65 per cent. ^1H NMR (δ/ppm): 0·88 (t, $-CH_3$, 6 H), 1·30 ($-CH_2-$, 56 H), 3·95 (t, $-O-CH_2-$, 8 H), 6·75–7·50 (C_6H_4, 16 H). IR (KBr, cm^{-1}): 2920, 2851, 1609, 1518, 1250, 839, 826, 806, 785.

1,7-Bis(4-(4′-n-tetradecyloxyphenylethynyl)phenoxy) heptane (14OTO7OTO14). Colourless fine crystals from methanol–chloroform. Yield: 57 per cent. ^1H NMR (δ/ppm): 0·88 (t, $-CH_3$, 6 H), 1·30 ($-CH_2-$, 58 H), 3·95 (t, $-O-CH_2-$, 8 H), 6·75–7·50 (C_6H_4, 16 H). IR (KBr, cm^{-1}): 2955, 2920, 2851, 1611, 1518, 1250, 841, 826, 787.

1,8-Bis(4-(4′-n-tetradecyloxyphenylethynyl)phenoxy) octane (14OTO8OTO14). Colourless fine crystals from chloroform. Yield: 49 per cent. ^1H NMR (δ/ppm): 0·88 (t, $-CH_3$, 6 H), 1·30 ($-CH_2-$, 60 H), 3·95 (t, $-O-CH_2-$, 8 H), 6·75–7·50 (C_6H_4, 16 H). IR (KBr, cm^{-1}): 2953, 2919, 2851, 1609, 1518, 1250, 839, 826, 783.

1,9-Bis(4-(4′-n-tetradecyloxyphenylethynyl)phenoxy) nonane (14OTO9OTO14). Colourless fine crystals from chloroform. Yield: 40 per cent. ^1H NMR (δ/ppm): 0·88 (t, $-CH_3$, 6 H), 1·30 ($-CH_2-$, 62 H), 3·95 (t, $-O-CH_2-$, 8 H), 6·75–7·50 (C_6H_4, 16 H). IR (KBr, cm^{-1}): 2955, 2920, 2851, 1611, 1518, 1254, 1175, 841, 826.

1,10-Bis(4-(4′-n-tetradecyloxyphenylethynyl) phenoxy)decane (14OTO10OTO14). Colourless fine crystals from chloroform. Yield: 66 per cent. ^1H NMR (δ/ppm): 0·88 (t, $-CH_3$, 6 H), 1·30 ($-CH_2-$, 64 H), 3·95 (t, $-O-CH_2-$, 8 H), 6·75–7·50 (C_6H_4, 16 H). IR (KBr, cm^{-1}): 2955, 2920, 2851, 1609, 1518, 1250, 839, 826, 785.

3. Results

3.1. *Phase identification*

Among the homologous series studied, TO*m*OT did not show any polymorphism, while the dimers with alkoxy terminal groups (*n*OTO*m*OTO*n*) exhibited a wide variety of phases, both crystalline and liquid crystalline. Assignment of mesophases was based on the study of the optical textures, mutual miscibilities and thermal analyses. Transition temperatures were determined by polarizing microscopy and were in excellent agreement with those made by DSC, deviations being less than 1°C. Data concerning thermal behaviour of the studied dimers are summarized in tables 1–4. All the observed mesophases were found in binary mixtures of two of the dimers, 6OTO6OTO6 and 10OTO6OTO10 (see figure 1), which facilitated the phase assignment.

Nematic phases (N) were detected only in the series with shorter terminal groups (6OTO*m*OTO6), corresponding to the general rules found for dimeric liquid crystals [8]. Mobile schlieren (see figure 2) or homeotropic textures were observed. Homeotropic textures could be easily transformed to the flashing schlieren texture with slight pressure on the glass slides. In many instances, free droplets exhibited a single point disclination in the centre of the droplet with four twisted dark brushes (see, for example, figure 4.17 in [18]).

On cooling the droplets of 6OTO6OTO6 from the nematic phase, the schlieren texture disappeared or became less bright at *c.* 191·0°C; the droplets appeared almost isotropic. On further cooling, a region with a perfect Maltese cross appeared and rapidly expanded from the centre of the droplet at 190·6–190·3°C. Accordingly, homeotropic textures developed in samples placed between glass slides. DSC measurements did not detect any change in the baseline related to this process. On further cooling, the next transition was detected at *c.* 186°C. Below this temperature, the droplets became terrace-shaped with flat tops and well-defined cliffs, often being decorated by the focal-conic domains. This transition was clearly detected by DSC (see figure 5(*d*)). The lower temperature phase was assigned as smectic A, while assignment of the intermediate temperature phase is less clear. The most characteristic feature of this 'intermediate phase' (IP) was the strong tendency to spontaneous alignment. When samples were placed between slides, only homeotropic textures were observed, both on heating and cooling, irrespective of the texture of the preceding phase. Free droplets (independent of their size or shape) exhibited the non-distorted radial (or close to this) distribution of local optical axes, judging from the corresponding interference pattern (see figure 3). Definitive textures were obtained only from the samples that were prepared by slow cooling nematic slabs with a uniform parallel alignment (using rubbed glass plates as substrates). Elongated focal-conic domains were observed (see figure 4). The latter feature is typical for layered phases. At the same time, the viscoelastic properties of this phase were similar to the nematic phase. Free droplets were as fluid as nematics, their surface was smooth and they could not be spread into free suspended films, whereas the smectic droplets were less fluid, terrace-shaped and could be easily spread into films of arbitrary thickness.

Table 1. Thermodynamic parameters of melting for the dimeric tolans of the TO*m*OT series.

Dimer	T_m/°C[a]	ΔH_m/kJ mol^{-1}	ΔS_m/J mol^{-1} K^{-1}
TO6OT	151(133)	63	149
TO7OT	114(83)	56	144
TO8OT	145(128)	73	174
TO9OT	108(89)	53	138
TO10OT	141(119)	80	194

[a] Data from the cooling cycle are given in parentheses.

In addition to the dimers of the 6OTO*m*OTO6 series, smectic A (S_A) phases were also found in the dimers 10OTO7OTO10 and 10OTO9OTO10, exhibiting homeotropic or focal-conic textures (see figure 6). Homeotropic textures typically indicate the optical uniaxiality of the corresponding phase [19]. Taking into account the terrace-like appearance of the free droplets, the viscoelastic properties and the position of this smectic in the phase diagram, the proposed assignment seems the most probable.

A smectic C (S_C) phase was found in the series with long terminal substituents (10OTO*m*OTO10 and 14OTO*m*OTO14). Schlieren textures were the most typical observed (see figure 7). On cooling a film of 10OTO7OTO10, as well as those of binary mixtures, the schlieren texture developed from homeotropic regions of smectic A, indicative of the smectic A–smectic C transition [19]. DCS measurements did not detect any signal at the corresponding temperatures, in agreement with the numerous empirical and theoretical findings about the continuous nature of this transition [18].

The Smectic B (S_B) phase was identified in 10OTO9OTO10 and 6OTO6OTO6 (just before crystallization). It appeared also in a broad range of temperature and concentration in the binary mixtures (see figure 1). Similar to the S_A phase, it exhibited a homeotropic texture, but was essentially less fluid (like wax). Being affected by the shear stress, the homeotropic film exhibited a birefringent fine-grain texture, as well as numerous cracks. An abrupt change in the shape of free droplets occurred during the $S_A \rightarrow S_B$ transition, often being accompanied by a glide and spreading of the material. All those observations are in agreement with the proposed assignment. It is not possible at present to specify whether it is the hexatic B or crystal B phase.

The lower temperature mesophases of the dimers belonging to the 10OTO*m*OTO10 and 14OTO*m*OTO14 series exhibited various textures (see figures 8–11), with the absence of homeotropic regions being their common feature. One can propose that this is due to an intrinsic biaxiality of these phases. Comparing the observed textures with the available literature data [19], the corresponding phases could be assigned as the tilted hexatic smectics F or I. Schlieren textures were characteristic of the smectic F phase, but mosaic patterns were also observed. Since the smectic I phase differs from the smectic F only by the tilt direction relative to the local

Table 2. Thermodynamical parameters of the phase transitions of the dimeric tolans of the 6OTO*m*OTO6 series[a].

Dimer	Cr_1	→(←)	Cr_2	→(←)	Cr_3	→(←)	S_B	→(←)	S_A	→(←)	IP	→(←)	N	→(←)	I	$\Sigma\Delta H_{trans}$ $\Sigma\Delta S_{trans}$
6OTO6OTO6	●	51(–)[c] [10; 31]	●	125·5(–)[d] [19; 49]	●	176(164) [47; 105]	○	–(165)[e]	●	186(186) [1·3; 2·9]	●	190·5(190·5)[f]	●	196(195) [8·7; 19]	●	85 *205*
6OTO7OTO6	●	36(32)[e]	●	39(34)[e] [9·2; 30]	●	143(128) [63; 151]					○	–(134)[f]	●	157(155) [3·4; 7·9]	●	75 *190*
6OTO8OTO6	●	49(44) [9·9; 31]	●	147(140) [31; 73]	●	161(152) [40; 92]			○	–(155·5) [(0·9); (2·1)]	○	–(165)[f]	●	177(176) [9·1; 20]	●	90 *220*
6OTO9OTO6	●	37(29)[e]	●	39(33)[e] [7·8; 25]	●	134(108) [65; 159]					○	–(116)[f]	●	152(149) [4·3; 10·0]	●	75 *195*
6OTO10OTO6	●	49(44) [9·6; 30]	●	148(141) [46; 109]	●	158(149) [48; 111]							●	167(166) [9·5; 22]	●	105 *270*

[a] T_{trans}(°C), [ΔH_{trans}(kJ mol^{-1}); ΔS_{trans}(J mol^{-1} K^{-1})], respectively. Data are obtained from DSC measurements, unless otherwise noted.

[b] Phase specification: Cr_1–Cr_3–crystalline phases, S_B–smectic B, S_A–smectic A, IP–intermediate phase, N–nematic, I–isotropic liquid. ●–enantiotropic phase, ○–monotropic phase.

[c] No crystallization at examined cooling rates, recovered after several days exposure at room temperature.

[d] No crystallization at examined cooling rates, appeared again on heating.

[e] Partly resolved doublet on the DSC chart. ΔH and ΔS are given for the sum of two transitions.

[f] Not detected by DSC, temperature was taken from polarizing microscopic observations.

Table 3. Thermodynamical parameters of the phase transitions of the dimeric tolans of the 10OTO*m*OTO10 series[a].

Dimer	Cr_1	→(←)	Cr_2	→(←)	Cr_3	→(←)	Cr_4	→(←)	S_1	→(←)	S_2	S_B	→(←)	S_C	S_A	→(←)	I	$\Sigma\Delta H_{trans}$ $\Sigma\Delta S_{trans}$
10OTO6OTO10	●	110(93) [22; 57]	●	117(95) [18; 46]	●	152(150·5) [7·0; 17]	●	157(152) [29; 67]	●	166·5(166)[c]	●		174(173·5) [10·5; 24]	●		187·5(186·5) [22; 47]	●	110 *240*
10OTO7OTO10	●	106(92)[d] [22; 59]	●					131(113) [62(49); 153(128)]	○	–(127)[c]	○		–(128) [(12); (30)]	●[e]	●	146(145) [12; 29]	●	95 *240*
10OTO8OTO10	●	109(97)[f] [23; 59]	●	137(130) [40; 99]	●			145(139) [19; 47]	●				161(159) [11; 25]	●		169(165) [23; 51]	●	115 *280*
10OTO9OTO10	●	108(102) [21; 54]	●					124(108) [45; 112]				●	128(126) [13; 33]		●	137(133) [12; 29]	●	90 *230*
10OTO10OTO10	●	111(106) [23; 61]	●	137(131) [33; 80]	●			150(145) [32; 75]			●					155(152) [31; 72]	●	120 *290*

[a] T_{trans}(°C), [ΔH_{trans}(kJ mol^{-1}); ΔS_{trans}(J mol^{-1} K^{-1})], respectively. Data are obtained from DSC measurements, unless otherwise noted.

[b] Phase specification: Cr_1–Cr_4–crystalline phases, S_1–smectic with schlieren texture, S_2–smectic with mosaic texture, S_B–smectic B, S_C–smectic C, S_A–smectic A, I–isotropic liquid; ●–enantiotropic phase, ○–monotropic phase.

[c] Not detected by DSC, temperature was taken from polarizing microscopic observations.

[d] Metastable crystalline phase appeared on cooling below 100°C.

[e] $T_{S_CS_A} = 139$°C, both on heating and cooling.

[f] Metastable crystalline phase appeared on cooling below 105°C.

Table 4. Thermodynamical parameters of the phase transitions of the dimeric tolans of the 14OTO*m*OTO14 series[a].

Dimer	Phase[b] Cr_1	$\rightarrow(\leftarrow)$	Cr_2	$\rightarrow(\leftarrow)$	Cr_3	$\rightarrow(\leftarrow)$	S_2	$\rightarrow(\leftarrow)$	S_C	$\rightarrow(\leftarrow)$	I	$\Sigma\Delta H_{trans}$ $\Sigma\Delta S_{trans}$
14OTO6OTO14	●	122(111) [56; 140]	●	137(131) [19; 46]	●	146(140) [17; 41]	●	162(160) [9·0; 21]	●	180(177) [23; 49]	●	125 *295*
14OTO7OTO14	●					123(113)[c] [90; 227]	●	127(125) [13; 33]	●	145(142) [18; 43]	●	120 *305*
14OTO8OTO14	●	125(121) [37; 94]	●	< 131[d]	●	135(125) [66; 163]	●	156(153) [13; 30]	●	164(161) [28; 63]	●	145 *350*
14OTO9OTO14	●					121(106) [98; 249]	●	131(128) [17; 42]	●	138(135) [22; 55]	●	135 *345*
14OTO10OTO14	●	126(122) [39; 97]	●	< 135[e]	●	138(129) [72; 176]	●			154(151) [44; 102]	●	155 *375*

[a] T_{trans}(°C), [ΔH_{trans}(kJ mol^{-1}); ΔS_{trans}(J mol^{-1} K^{-1})], respectively. Data are obtained from DSC measurements, unless otherwise noted.

[b] Phase specification: Cr_1–Cr_3–crystalline phases, S_2–smectic with mosaic texture, S_C–smectic C, I–isotropic liquid; ●–enantiotropic phase, ○–monotropic phase.

[c] Metastable crystalline phase appeared on cooling between 113 and 114°C.

[d] Cr_2 melts at 131°C.

[e] Cr_2 melts at 135°C.

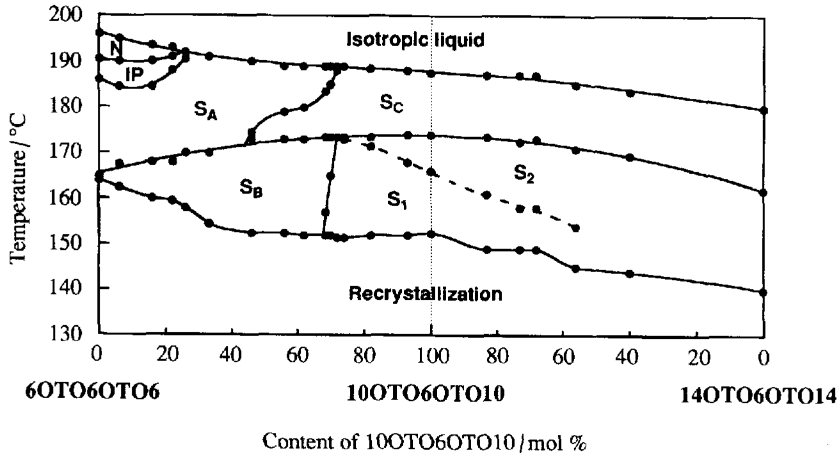

Figure 1. Combined phase diagrams of 6OTO6OTO6:10OTO6OTO10 and 10OTO6OTO10:14OTO6OTO14 mixtures.

hexagonal lattice, they exhibit a similar texture. Moreover, a number of novel modulated hexatic phases of complex structures were recently reported [20]. Obviously, the final assignment can be made only after an X-ray analysis of aligned samples. It is worth noting that the direct transition from the smectic C to the lower temperature smectic phase with the schlieren texture was observed only for 10OTO8OTO10. In all other cases, the smectic C phase was replaced by phases consisting of uniformly coloured domains with sharply defined zigzag boundaries (see figure 8). Disclinations of the preceding smectic C phase transformed into six- or five-armed stars, similar to those found in free-standing films of the smectic I phase [21]. On further cooling of 10OTO6OTO10 and 10OTO7OTO10, zigzag lines smoothed, while the centres of the star defects transformed again into disclinations of integral strengths, finally yielding schlieren textures (see figure 9), but were coarser when compared to the S_C phase. Both textures could be reversibly transformed to each other by varying the temperature. To reflect this peculiarity, they are denoted as S_1 (schlieren texture) and S_2 (mosaic texture). Although $S_1 \leftrightarrow S_2$ transformations took place at certain temperatures, they proceeded smoothly and were not detected by DSC. At present, it is hard to conclude whether these are distinct phases or modifications of the same phase. A somewhat different picture took place in the 14OTO*m*OTO14 series. Mosaic textures (for example, see figure 8) were observed in the vicinity of the $S_C \leftrightarrow S_2$ transition. On further cooling, smectic films appeared as uniformly coloured domains with cone-like dark arms. These arms originated from the domain boundaries and rotated with rotation of the nicols, some clockwise, others anti-clockwise (see figures 10 and 11), resembling optical patterns of so-called 'developable domains' in columnar phases [22]. A phase transition between the S_B and S_1 phases was detected in the 30:70 mol % mixture of 6OTO6OTO6 and 10OTO6OTO10. Schlieren textures of the S_1 phase developed from the homeotropic regions of the S_B phase and vice versa, resembling features of the $S_A \leftrightarrow S_C$ transition. Similar by, it was not detected by DSC.

3.2. *Double melting*

Double melting was found in two compounds of the studied series, namely 14OTO8OTO14 and 14OTO10OTO14. Two peaks on the DSC charts corresponded to the crystal–mesophase transitions. On rapid heating, melting occurred at lower temperatures, whereas the slower scanning rates revealed the second transition that became predominant at the heating rate of 2°C min^{-1} (see figure 12). In all cases, the sum of the enthalpies of both transitions was constant. According to microscopic observations, the crystal phase and mesophase coexisted in the temperature range between the two peaks. When heating rates were more than 20°C min^{-1}, the crystal–mesophase transition proceeded completely at the lower temperature. However, if the sample was then held at a constant temperature between the two melting endotherms, the new crystal phase (Cr_3) began to grow, replacing the mesophase. On further heating, this phase melted at the temperature corresponding to the second peak. When slow heating rates (<1°C min^{-1}) were applied, the Cr_3 phase appeared immediately after the $Cr_2 \rightarrow S_2$ transition. Since these endothermic (melting) and exothermic (crystallization) processes occurred almost simultaneously, they were not detected by DSC. According to these observations, the Cr_3 phase seems thermodynamically stable in a range of several degrees below the melting point. However, the direct $Cr_2 \rightarrow Cr_3$ transition is likely to be suppressed by kinetic considerations. Only melting of the Cr_2 phase and formation of the Cr_3 phase from the supercooled mesophase were observed. It is not possible at present to establish exactly the temperatures of the $Cr_2 \leftrightarrow Cr_3$ transitions for these dimers. For comparison, the corresponding solid–solid transitions were found at temperatures more than 20°C below the melting points of the metastable phases in the case of discotic copper β-diketonates [23].

3.3. *Regularities in the thermodynamical parameters of the phase transitions*

Similar to other dimesogenic compounds, as well as main-chain polymeric liquid crystals [24], the regular odd–even alternation of the melting and clearing points with the number of methylene units, *n*, in the central spacer was observed (see figures 13 and 14). This effect was previously studied both theoretically and experimentally, and its detailed treatment can be found elsewhere [4, 8]. Similarly to most liquid crystals, enthalpies of the nematic–isotropic transitions were less than those of the smectic A (or C)–isotropic liquid transitions by several times. In turn, the $S_A(S_C)$–I were weaker than the $S_2 \leftrightarrow I$ transitions. It is worth noting that the temperatures and enthalpies of the $Cr_1 \leftrightarrow Cr_2$ transitions (see figures 13 and 14, squares) apparently correlated with the number of methylene units in the terminal chains. Surprisingly, enthalpies of melting (except for the non-mesomorphic series TO*m*OT) showed a striking odd–even effect of an opposite sign (see figure 14, filled circles). In an extreme example, ΔH_m of 14OTO6OTO14 was 5·3 times weaker than the ΔH_m of the neighbouring 14OTO7OTO14 (see table 4). In contrast to the other transitions, no obvious correlations between the melting enthalpies and the lengths of the terminal chains were observed. However, total transition enthalpies exhibited a regular odd–even alternation and an almost linear relation with the number of methylene units in terminal groups (see figure 15, filled circles), with the TO*m*OT series also obeying this rule. The solubilities of the dimeric tolans in chloroform demonstrated the same dependence in a reversed log scale (see figure 15, open circles).

4. Discussion

In the present study, only some features of mesomorphic behaviour could be briefly discussed. First, the strange 'intermediate phase'. If was not possible to define it unambiguously. Some of the observed phenomena might possibly be considered from the position of the 'frustrated smectic' model [18], which relates changes in the structure of mesophases with the interaction of units having incompatible lengths. This model was successfully applied to polar mesogens [25] and unsymmetrically substituted dimers [7], but structural data are necessary to support this. Obviously, any of the possible models in the future should explain the nematic-like character and self-alignment of this phase, as well as peculiarities of the phase transitions. Another feature of the system studied was the appearance of 'developable domains' in the S_2 phase (14OTO*m*OTO14 series). Similar textures were observed in layered phases [26], where they formed modulated two-dimensional structures, so-called 'antiphases' [18, 20]. Probably, a similar phenomenon could also occur in these dimeric tolans.

Several apparent correlations between the chemical structure and mesomorphic behaviour of the dimeric tolans were found. Following the common trend in liquid crystals, shorter terminal groups (OC_6H_{13}, in the

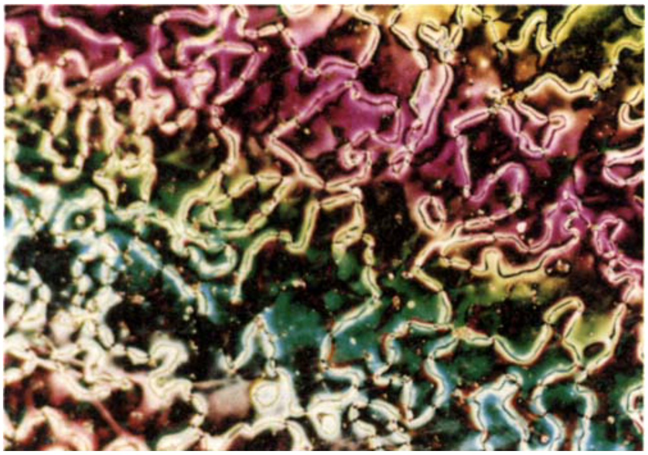

Figure 2. Nematic phase of 6OTO6OTO6 at 195·2°C (heating, crossed nicols, × 225).

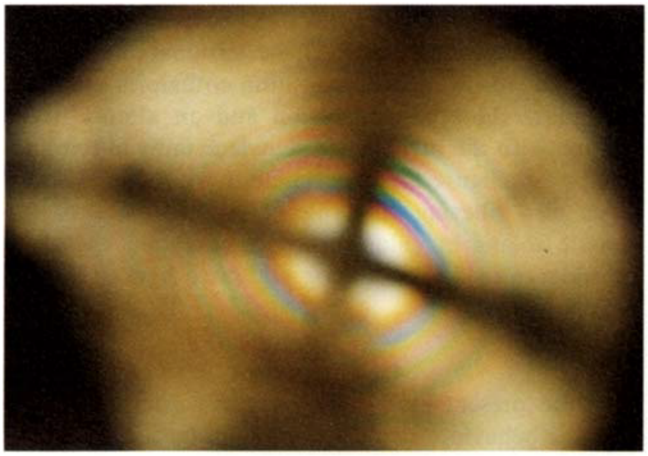

Figure 3. 'Intermediate phase' in a free droplet of 6OTO6OTO6 at 190·0°C (cooling, crossed nicols, × 90).

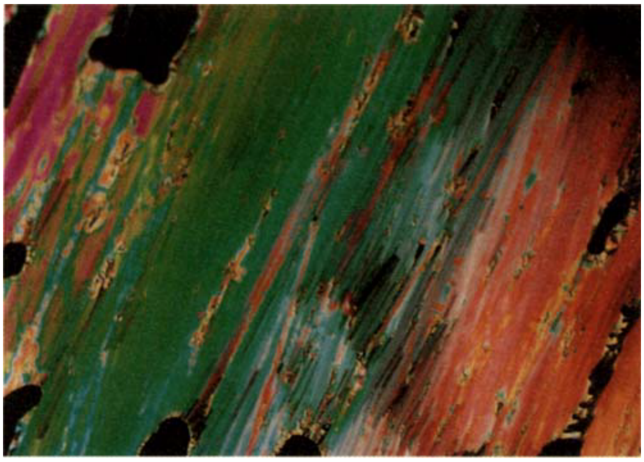

Figure 4. 'Intermediate phase' of 6OTO6OTO6 in a slab with parallel alignment at 189·8°C (cooling, crossed nicols, × 225). Focal domains are aligned along to the rubbing direction.

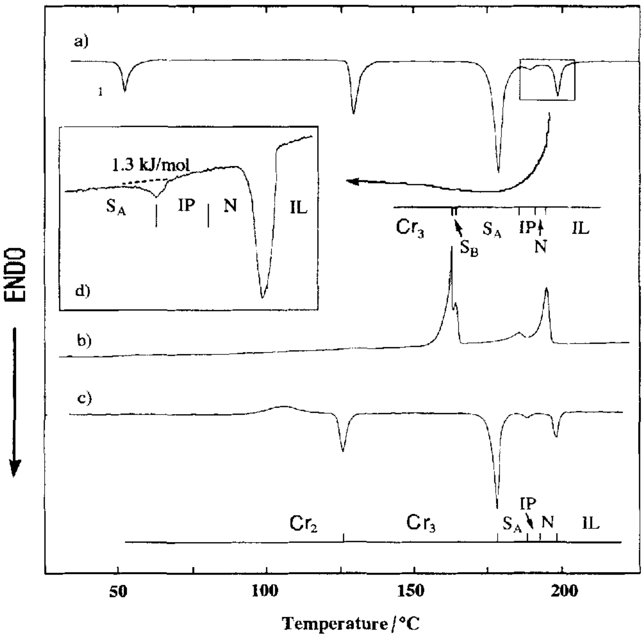

Figure 5. DSC thermograms of 6OTO6OTO6: (*a*) first heating, 10°C min^{-1}, (*b*) cooling, 5°C min^{-1}, (*c*) second heating, 5°C min^{-1}, (*d*) the mesophase region, obtained with a heating rate of 1°C min^{-1}.

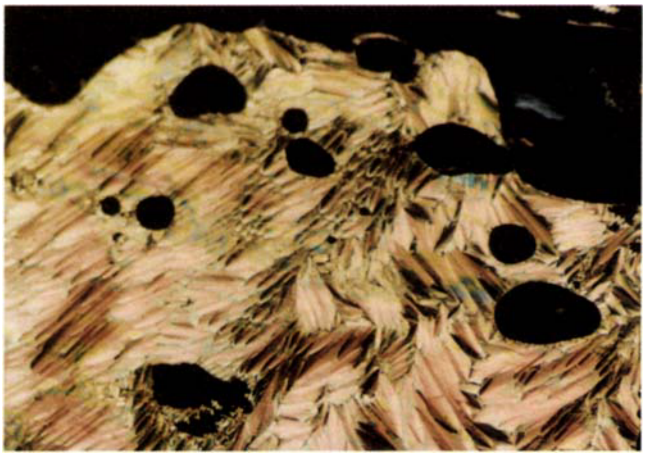

Figure 6. Smectic A phase of 6OTO6OTO6 at 185·2°C (heating, crossed nicols, × 225).

present case) promoted nematic phases, while longer substituents favoured smectic phases. Moreover, the dimeric tolans showed a tendency to form tilted smectics with a lengthening of the terminal groups. Figure 1 gives a demonstrative example of the observed correlation. Nematics existed in neat 6OTO6OTO6, and then this phase (and simultaneously an 'intermediate phase') disappeared when the content of 10OTO6OTO10 exceeded 26 %. In turn, the non-tilted smectics A and B were finally replaced by S_C and S_1 phases in the range be-

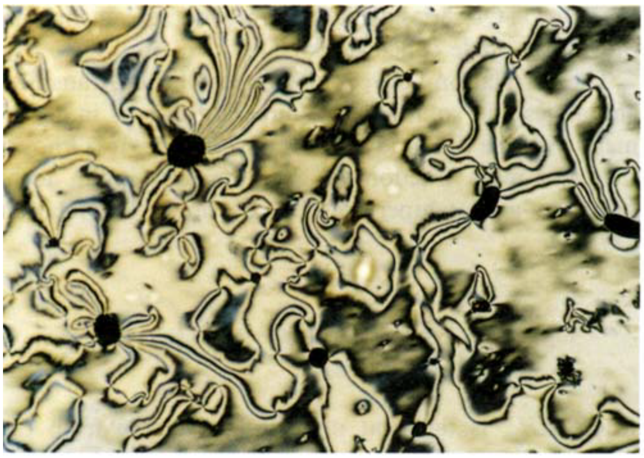

Figure 7. Smectic C phase of 10OTO6OTO10 at 185·0°C (cooling, crossed nicols, × 225).

Figure 8. Smectic S_2 phase of 10OTO6OTO10 at 172·6°C (the same sample, cooling, crossed nicols, × 225).

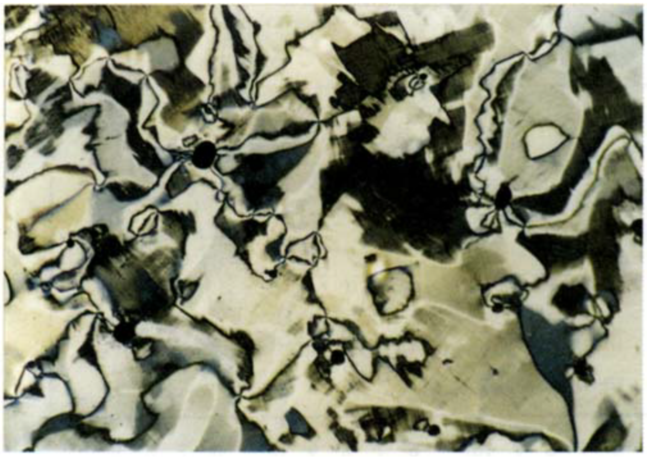

Figure 9. Smectic S_1 phase of 10OTO6OTO10 at 160·0°C (the same sample, cooling, crossed nicols, × 225).

Figure 10. Smectic S_2 phase of 14OTO6OTO14 at 161·4°C (cooling, crossed nicols, × 225).

Figure 11. Smectic S_2 phase of 14OTO6OTO14 at 161·4°C, the same sample after rotating of nicols by 30° clockwise (cooling, crossed nicols, × 225).

tween 68 and 72 % of 10OTO6OTO10. A 'switching' sequence of orthogonal and tilted phases S_A–S_C–S_B–S_1 was observed in the same sample in this range of concentration. Only tilted smectics occurred for the 10OTO6OTO10 : 14OTO6OTO14 system. Since the central parts of the dimers in these mixtures were the same, one can attribute the observed phenomena to the influence of terminal groups. An odd–even effect was exhibited by the dimers of the 10OTO*m*OTO10 series, with non-tilted phases being detected only in the odd members. The influence of the bridging substituents was similar to that in liquid crystalline polymers [24]. Increasing the length of the spacer led to a decrease in the clearing and melting points and a narrowing of the temperature range of the mesophases. Furthermore, longer spacers promoted nematic phases in the

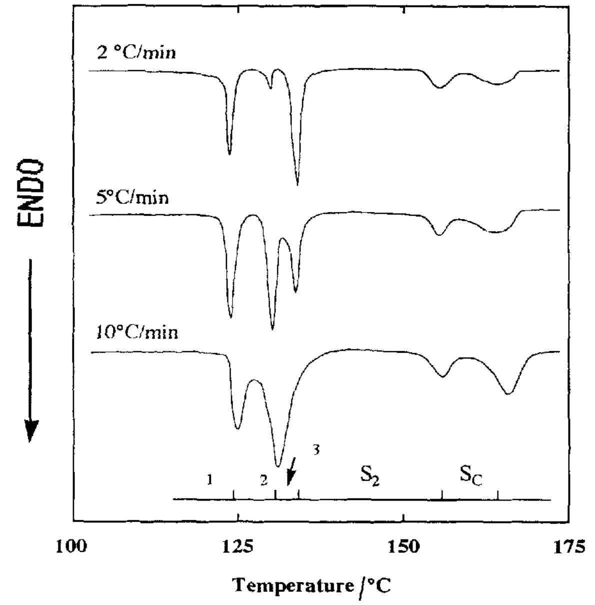

Figure 12. DSC thermograms of 14OTO8OTO14, obtained at different heating rates. (1–3 indicate crystals 1–3).

6OTO*m*OTO6 series, which is in a good agreement with previously made conclusions [8].

The correlation between the values of total transition enthalpies and solubilities of dimeric tolans is in agreement with the thermodynamics of solutions. It is known that the mole fraction of a solute (x_2) in an ideal solutions at a temperture $T' > T''$ obeys the relation [27]

$$\log\frac{x_2''}{x_2'} = \int_{T''}^{T'} \frac{\Delta H_m(T)}{RT^2}\,dT \approx -\frac{\Delta H_m}{R}\left(\frac{1}{T''}-\frac{1}{T'}\right)$$

where ΔH_m is the heat of melting. Judging from the established correlation between $-\log x_2$ and $\sum \Delta H_{trans}$ ($R^2 = 0{\cdot}879$), the sum of the enthalpies of all transitions of the polymorphic compound virtually replaces the melting enthalpy of the ordinary substance in thermodynamical expressions. In this respect, polymorphic compounds undergo a kind of stepwise melting. Odd–even alternations in the spacer gave the main relative contribution to the change of both solubilities and total transition enthalpies.

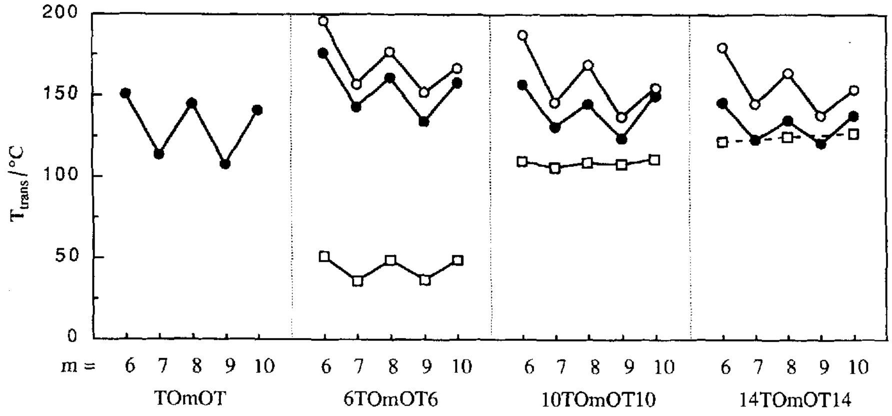

Figure 13. Transition temperatures as a function of the length of the aliphatic spacer: ○ mesophase–isotropic liquid, ● crystal–mesophase (or isotropic liquid), □ crystal 1–crystal 2.

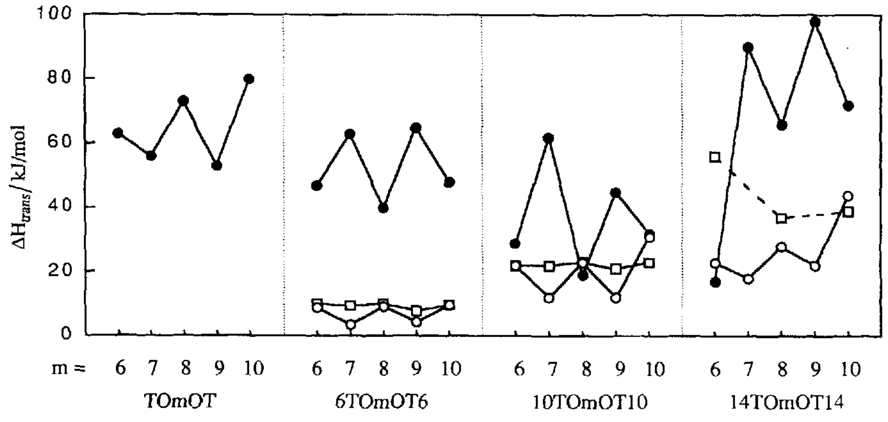

Figure 14. Transition enthalpies as a function of the length of the aliphatic spacer: ○ mesophase–isotropic liquid, ● crystal–mesophase (or isotropic liquid), □ crystal 1–crystal 2.

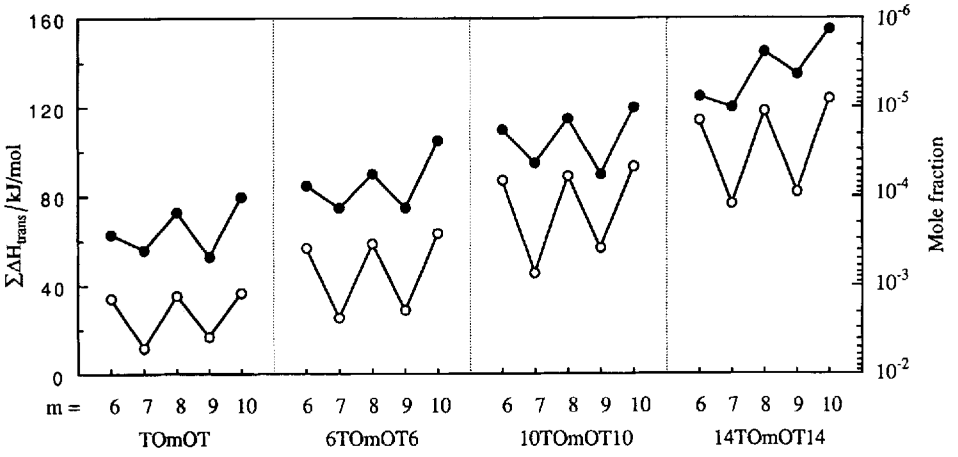

Figure 15. Correlations between the total transition enthalpies (●) and solubilities (○) of the dimeric tolans.

5. Conclusions

A novel system of dimeric liquid crystals with tolan (diphenylacetylene) mesogenes was synthesized and studied by thermal and optical methods. The majority of the obtained α,ω-bis(4-(4′-*n*-alkoxyphenylethynyl)-phenoxy)alkanes exhibited a high degree of polymorphism. A general trend to form tilted smectic phases with an increasing size of the terminal alkoxy groups was found. Differences between melting and clearing points decreased with the lengthening of the spacer. An odd–even effect of the transitional parameters was clearly observed. Taking into account the simple symmetric structures, as well as the chemical and thermal stability of the dimers, they may be applicable in the future as convenient model compounds in the field of polymer science. The phenomenon of self-alignment that occurred in the 'intermediate phase' between the nematic and smectic phases could possibly be of some practical importance, provided its nature could be elucidated.

The authors are grateful to Prof. T. Ikeda for his permission to perform the optical observations, and helpful discussion.

References

[1] Griffin, A. C., and Britt, T. R., 1981, *J. Am. chem. Soc.*, **103**, 4957.

[2] Watanabe, J., Komura, H., and Niiori, T., 1993, *Liq. Cryst.*, **13**, 455.

[3] Abe, A., and Furuya, H., 1989, *Macromolecules*, **22**, 2982.

[4] Abe, A., Furuya, H., Shimizu, R. N., and Nam, S. Y., 1995, *Macromolecules*, **28**, 96 and references therein.

[5] Praefke, K., Kohne, B., Gündogan, B., Singer, D., Demus, D., Diele, S., Pelzl, G., and Bakowsky, U., 1991, *Molec. Cryst. liq. Cryst.*, **198**, 393.

[6] Hardouin, F., Archard, M. F., Jin, J.-I., Shin, J.-W., and Yun, Y.-K., 1994, *J. Phys. II France*, **4**, 627.

[7] Hardouin, F., Archard, M. F., Jin, J.-L., and Jun, Y.-K., 1995, *J. Phys. II France*, **5**, 927.

[8] Date, R. W., Imrie, C. T., Luckhurst, G. R., and Seddon, J. M., 1992, *Liq. Cryst.*, **12**, 203.

[9] Rozhanskii, I. L., Tomita, I., and Endo, T., 1996, *Macromolecules*, **29**, 1934.

[10] Malthête, J., Leclercq, M., Dvolaitzky, M., Gabard, J., Billard, J., Pontikis, V., and Jacques, J., 1973, *Molec. Cryst. liq. Cryst.*, **23**, 233.

[11] Dubois, J. C., Zann, A., and Couttet, A., 1974, *Molec. Cryst. liq. Cryst.*, **27**, 187.

[12] Kantor, S. W., and Sung, T.-C., 1993, *Macromolecules*, **26**, 3758.

[13] Al-Dujaili, A. H., Jenkins, A. D., and Walton, D. R. M., 1984, *J. Polym. Sci., Polym. Chem. Ed.*, **22**, 3129.

[14] Al-Dujaili, A. H., Jenkins, A. D., and Walton, D. R. M., 1988, *Molec. Cryst. liq. Cryst.*, **164**, 25.

[15] Brandsma, V., and Verkruijsse, H. D., 1981, *Synthesis of Acetylenes, Allenes and Cumulenes* (Elsevier), pp. 55–56.

[16] Swiss, K. A., Hinkley, W., Maryanoff, C. A., and Liotta, D. C., 1992, *Synthesis*, 127.

[17] Takahashi, S., Kuroyama, Y., Sonogashira, K., and Hagihara, N., 1980, *Synthesis*, 627.

[18] De Gennes, P. G., and Prost, J., 1993, *The Physics of Liquid Crystals* (Clarendon Press).

[19] Gray, G. W., and Goodby, J. W., 1984, *Smectic Liquid Crystals—Textures and Structures* (Leonard-Hill).

[20] Date, R. W., Luckhurst, G. R., Shuman, M., and Seddon, J. M., 1995, *J. Phys. II France*, **5**, 587.

[21] Dierker, S. B., Pindak, R., and Meyer, R. B., 1986, *Phys. Rev. Lett.*, **56**, 1819.

[22] Oswald, P., and Kléman, M., 1981, *J. Phys., France*, **42**, 1461.

[23] Ohta, K., Muroki, H., Hatada, K.-I., Yamamoto, I., and Matsuzaki, K., 1985, *Molec. Cryst. liq. Cryst.*, **130**, 249.

[24] Ober, Ch. K., Jin, J.-I., and Lenz, R. W., 1984, *Advances in Polymer Sciense*, edited by M. Gordon (Springer-Verlag), Vol. 59, p. 103.

[25] Prost, J., and Barois, P., 1983, *J. chem. Phys.*, **80**, 65.

[26] Ribeiro, A. C., Dreyer, A., Oswald, L., Nicoud, J. F., Soldera, A., Guillon, D., and Galerne, Y., 1994, *J. Phys. II France*, **4**, 407.

[27] Lewis, G. N., and Randall, M., 1961, *Thermodynamics* (McGraw-Hill).